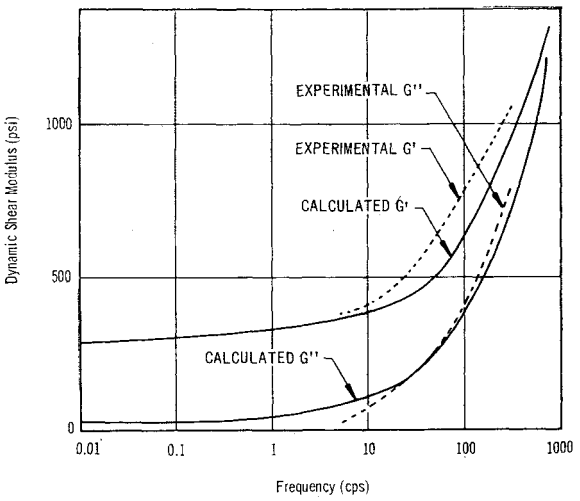

Fig. 5 Dynamic shear modulus vs frequency real (G') and imaginary (G'') parts.

cation within 0.001 sec for accurate viscoelastic transformations was indicated.

During this investigation, the stress relation functions were evaluated. The results of these determinations were used satisfactorily to describe the time dependency of the propellant. This enabled an accurate prediction of the dynamic shear modulus to be made, as is evidenced by the comparison of the calculated and the experimentally determined values.

References

[1] Saylak, D., "The design, fabrication, and evaluation of an end-bonded cylindrical tensile dumbbell for tensile testing composite rocket propellants," Chemical Propulsion Information Agency Bulletin of the 1st Meeting for the Working Group on Mechanical Behavior, p. 54 (December 1962); confidential.

[2] Gross, B., *Mathematical Structure of the Theories of Viscoelasticity* (Publications of the National Institute of Technology, Brazil, 1953), Chap. 3.

[3] Francis, E. C. and Cantey, D., "Solid propellant structural integrity investigation," Lockheed Propulsion Co. TR RTD-TDR-63-1 (May 24, 1963).

A Dynamical Model for Kordylewski Cloud Satellites

FREDERICK V. POHLE*
Adelphi University, Garden City, N. Y.

THE existence of additional natural satellites near the earth has been the object of observational searches[1]; no positive results were announced. In the earth-moon system it is known[2] that the Lagrangian equilateral triangular points (L_4, L_5) are stable points and that matter may remain for a long time in the regions close to such points. Thus it is natural to seek the existence of natural satellites in such regions, and a search was undertaken by K. Kordylewski of the Cracow Observatory in Poland a number of years ago. Success was announced[3–6] with the statement that a pair of thin cloud-like satellites was observed near each stable L point The observational difficulties are extremely great since the clouds are observable on only three nights a month for about two hours between December and April.[7] Although a search has been underway to detect meteoroids within the clouds, none as bright as the twelfth-magnitude has been detected up to the present time.

The existence of dust in the earth-moon space is well known,[8–10] and the object of the present note is to suggest a possible dynamical model[11] to explain the accumulation in the form of clouds observed by Kordylewski. A different explanation has been advanced[12] based on the motion of particles near the stable L points in the form of periodic orbits.

The present model assumes the existence of a small nucleus at the stable L point and the existence of dust moving in the region, near the L point. Since matter can accumulate near the L point, it is at least possible that a small mass, once captured, would remain near the stable point for an indefinite time. This is clearly an assumption at the present time, since the observations have not given positive evidence of the existence of a nucleus. The location of the L point in the earth-moon system is of course determined by the dimensions of that system. Nevertheless, the sphere of influence of the moon is too small for the moon to have an appreciable influence on dust particles near such an L point and, for purposes of a simplified presentation, the effect of the moon will be ignored; a more accurate analysis leads to the same conclusions. The analysis is similar in some respects to the explanation of the gegenschein[13] at the unstable L points (L_1, L_2, L_3).

It will be assumed that the nucleus, as well as the cloud near it, moves in a circular orbit about the earth at a distance equal to that of the lunar distance a in Fig. 1. The small mass is $m(x, y)$ and the plane of the orbit is the (x, y) plane. A general particle of the cloud is at (ξ, η, ζ), and the distance from the nucleus to any particle is r_2, which is small compared with a, and with r_1, the distance to the earth of mass M located at the origin; the ratio $m/M = \beta$ is assumed to be extremely small compared with unity.

The particle (ξ, η, ζ) is attracted by m and M but does not influence their motion; m is in uniform circular motion about M. The equations of motion of a typical dust particle can be written as

$$\begin{aligned} \ddot{\xi} &= -GM\xi/r_1^3 - Gm(\xi - x)/r_2^3 \\ \ddot{\eta} &= -GM\eta/r_1^3 - Gm(\eta - y)/r_2^3 \\ \ddot{\zeta} &= -GM\zeta/r_1^3 - Gm\zeta/r_2^3 \end{aligned} \tag{1}$$

where G is the gravitational constant and $r_1^2 = \xi^2 + \eta^2 + \zeta^2$, $r_2^2 = (\xi - x)^2 + (\eta - y)^2 + \zeta^2$; $x = a\cos(kt)$, $y = a\sin(kt)$, $k^2 = GM/a^3$.

The usual uniformly rotating reference system is now introduced in which m is a fixed point on the X axis; the unit of distance is chosen to be a, and the dimensionless time $\tau = kt$ is introduced as the new independent variable, with $' = d/d\tau$;

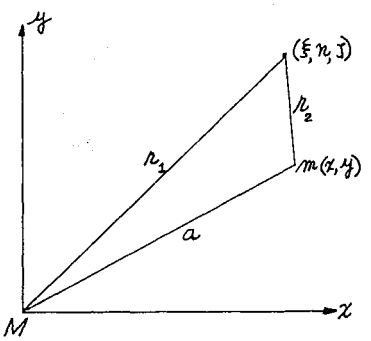

Fig. 1

Presented as Preprint 63-425 at the AIAA Astrodynamics Conference, New Haven, Conn., August 19–21, 1963; revision received July 16, 1964. The work reported upon here was begun at the Mathematics Research Center of the U. S. Army at the University of Wisconsin under Contract DA-11-022-ORD-2059 and was continued under the Air Force Office of Scientific Research Grant 598-64 at Adelphi University.

* Professor of Mathematics. Associate Fellow Member AIAA.

that is, we introduce the new variables by means of the substitutions

$$\begin{aligned} \xi &= a[X\cos\tau - Y\sin\tau] \\ \eta &= a[X\sin\tau + Y\cos\tau] \\ \zeta &= aZ \end{aligned} \tag{2}$$

In addition, we have the new relations $R_1^2 = X^2 + Y^2 + Z^2$ and $R_2^2 = (X-1)^2 + Y^2 + Z^2$ with $(\beta, R_1, R_2 > 0)$. The final forms of the differential equations are

$$\left.\begin{aligned} X'' - 2Y' - X &= -X/R_1^3 - \beta(X-1)/R_2^3 \\ Y'' + 2X' - Y &= -Y/R_1^3 - \beta Y/R_2^3 \\ Z'' &= -Z/R_1^3 - \beta Z/R_2^3 \end{aligned}\right\} \tag{3}$$

If Eqs. (3) are multiplied by X', Y', Z', respectively, and integrated, the usual form of the Jacobi integral will be obtained in the form

$$V^2 = (X')^2 + (Y')^2 + (Z')^2 = X^2 + Y^2 + (2/R_1) + (2\beta/R_2) - K \tag{4}$$

where K is a positive constant in further discussions. The discussions of the possible zero-velocity surfaces is simplified if cylindrical coordinates are introduced by means of the equations $X = 1 + \rho\cos\varphi$, $Y = \rho\sin\varphi$, and $Z = z$. Terms up to $0(\rho^2)$ will be retained in the analysis, and particular attention will be paid to those values of z which are small compared with the radial distance ρ. If $z = 0$, the Jacobi integral (4) can be written as

$$V^2 = 3\rho^2\cos^2\varphi + (2\beta/\rho) - K \tag{5}$$

If a particle is assumed to be at a given point (ρ_0, φ_0) with the speed V_0, then the constant K is fixed; if V is zero in Eq. (5), the curves will be the traces of the zero-velocity surfaces, if such surfaces exist.

If K is positive, it is possible for V to equal zero in Eq. (5) by proper choice of (ρ, φ); if V_0^2 is sufficiently large, then K is negative and it is not possible for V to vanish. In such cases, no surfaces of zero relative velocity exist.

It may be assumed that K has been determined to be positive and that we have set $V = 0$ to obtain the equation

$$3\rho^3\cos^2\varphi - K\rho + 2\beta = 0 \tag{6}$$

The cubic (6) in ρ has one real negative root since the leading coefficient and the constant term are positive; this root is of no physical interest. The remaining two roots are either conjugate complex roots or both positive, since the sum of all roots is zero; our interest is in the latter case, which requires that

$$\cos^2\varphi < K^3/(81\beta^2) \tag{7}$$

In the form of the inequality (7), two cases of immediate interest arise. In the first, if $K^3 > 81\beta^2$, then no restriction is placed on φ, since the inequality is always satisfied. It is, of course, assumed that K is positive in all cases. In the second case, if $K^3 < 81\beta^2$, then there is a restriction on φ, and not all regions for φ are admissible: only a small wedge-shaped region for which $\cos^2(\varphi) = K^3(81\beta^2) < 1$ will be an admissible region.

If $K^3 > 81\beta^2$, all angles are admissible, and the limiting case is reached for $K^3 = 81\beta^2$. The traces in two cases are shown in Fig. 2. The traces for the limiting cases are shown by the curves C_1; if K^3 is larger than $81\beta^2$, the traces are indicated by C_2. For such values of K there is a closed inner oval and a pair of curves that extend to infinity and have the asymptotic width $2(K/3)^{1/2}$. Thus, as K increases, the inner oval becomes smaller in size and the outer traces move outward. The regions of positive V^2 are outside the pair of curves and inside the oval; these regions are indicated by cross-hatched lines for C_2. A particle placed at a in Fig. 2 with $V_0 = 0$ will remain there according to the equations of

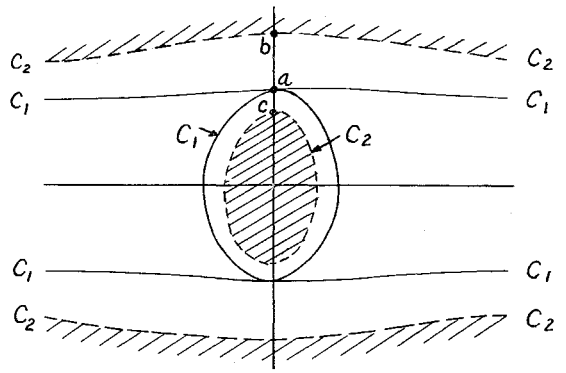

Fig. 2

motion; a particle placed at b will move outward, but a particle placed at c will move inward. If the initial speed V_0 is not zero, then a similar analysis can be made if we require that K^3 be at least $81\beta^2$.

If, however, V_0 is large enough, it is possible for K^3 to decrease and remain positive so that K^3 is less than $81\beta^2$ but greater than zero. The traces then change in form, and only certain ranges of φ are admitted, as shown in a typical case in Fig. 3. The regions of negative V^2 are inside the branches, and particles cannot enter such regions. The asymptotic width is still $2(K/3)^{1/2}$, but now K is smaller than in the previous case, and so the asymptotic width is also smaller.

In the present case, if a particle is placed in the admissible region with $V_0^2 > 0$, then, as a particle moves closer to the zero-V trace, its speed will decrease. The equations of motion of course determine the actual particle paths in the relative coordinate system. The acceleration is not zero on the zero-V curves but is normal to the curves and directed outward. The essential point is that some particles may approach to the zero-V curves and remain there for an appreciable time, and a slow accumulation of matter can take place near such curves. If K is smaller than before, the curve $V = 0$ is thinner and inside the one shown in Fig. 3. Thus, a narrow region of space $(z = 0)$ acts as an area where particles may move and accumulate slowly. Ultimately these particles will drift into other regions of space, but since there is a steady drift of such particles throughout the space, there will be new particles streaming into the region to replace those which may have moved away. This condition requires that the particle speeds be close to the orbital speeds at the L points, since K is small. If the initial speeds are large enough, then no zero-V surfaces can exist; this is reasonable since it indicates that the particle cannot be trapped or brought near to relative rest in the vicinity of the L point. The dynamical model that has been assumed therefore gives rise to the possibility that faint cloud-like patches may appear in the regions of the stable L points.

References

[1] Tombaugh, C. W., "Proposed geodetic triangulation from an unmanned orbital vehicle by means of satellite search technique," ARS Preprint 166-54 (November 1954).

[2] Moulton, F. R., *An Introduction to Celestial Mechanics* (The MacMillan Co., New York, 1958), 2nd ed., pp. 306–307.

[3] Sky Telescope, 10 (July 1961).

[4] Sky Telescope, 63, 83 (August 1961).

[5] Sky Telescope, 328 (December 1961).

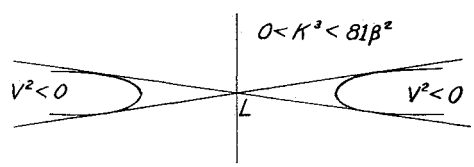

Fig. 3

[6] Kordylewski, K., "Photographische Untersuchungen des Librations-punktes L_5 im System Erde-Mond," Acta Astron. **11**, 165–169 (1961); also Cracow Observatory Reprint 46 (1961).
[7] Dauvillier, A., *Cosmic Dust* (George Newnes, Ltd., London, 1961), p. 31.
[8] Beard, D. B., "Interplanetary dust distribution," Astrophys. J. (1959).
[9] Singer, S. F., "Interplanetary dust near the earth," Nature **192**, 321–323 (October 1961).
[10] Whipple, F. L., "The dust cloud about the earth" Nature **192**, 127–128 (January 1961).
[11] Pohle, F. V., "The least density of a spherical swarm of particles, with an application to astronomical observations of K. Kordylewski," AIAA Preprint 63–425 (1963).
[12] Michael, W. H., Jr., "Consideration of the motion of a small body in the vicinity of the stable libration points of the earth-moon system," NASA TR R-160 (1963).
[13] Moulton, F. R., "A meteoric theory of the gegenschein," Astronom. J. **XXI**, 17–22 (1900).

Large Deflection of Sandwich Plates with Orthotropic Cores

A. M. ALWAN*
U. S. Naval Academy, Annapolis, Md.

Nomenclature

x, y, z	=	rectangular coordinates
a, b	=	length and width of sandwich plate
h	=	thickness of core
t	=	thickness of face layers
E, ν	=	Young's modulus of elasticity and Poisson's ratio
G_{xz}, G_{yz}	=	shear moduli of core
τ_{xz}, τ_{yz}	=	stresses in core
q	=	load per unit area
M_x, M_y, M_{xy}	=	bending and twisting moments per unit length
N_x, N_y, N_{xy}	=	stress resultants in middle plane of face layers per unit length
Q_x, Q_y	=	shear forces per unit length
u, v, w	=	displacements in x, y, and z directions
$\beta, \beta', \gamma, \gamma'$	=	generalized boundary displacements
$\lambda_1, \lambda_2, \lambda_3,$ λ_4, λ_5	=	Lagrangian multipliers

Introduction

THE problem of large deflection of sandwich plates has been investigated by several authors. Reissner[3] presented an exact analysis of finite deflections of sandwich plates, Wang[4] gave a general theory of large deflection of homogeneous and sandwich plates and shells, Hoff[5] and Eringen[6] each developed a theory of bending and buckling of sandwich plates. In all of the foregoing investigations the core and facings of the sandwich plates were assumed to be isotropic. In the present analysis the core is taken as an orthotropic honeycomb-type structure. It is felt that this type of core corresponds more exactly to the behavior of actual sandwich construction used in industry.

The sandwich plate shown in Fig. 1 is assumed to consist of two thin isotropic face layers, each, of thickness t separated by and bonded to an orthotropic core of thickness h. The usual assumptions for sandwich plates are adopted here, as in Ref. 3. In addition, the effect of the transverse normal stresses in the core is considered negligibly small compared with the effect of the transverse shear stresses on the over-all behavior of the plate.

Analysis

Since all the face-parallel core stresses are neglected, the face-parallel stress resultants of the composite plate are due to the stresses in the face layers only as shown in Fig. 2 and may be obtained as follows:

$$N_x = N_{xu} + N_{xl} \qquad N_y = N_{yu} + N_{yl}$$
$$N_{xy} = N_{xyu} + N_{xyl}$$

where the subscripts u and l refer to the upper and lower face layers, respectively.

The differential equations of equilibrium are[1]

$$\left.\begin{aligned} &\frac{\partial N_x}{\partial x} + \frac{\partial N_{xy}}{\partial y} = 0 \qquad \frac{\partial N_y}{\partial y} + \frac{\partial N_{xy}}{\partial x} = 0 \\ &\frac{\partial Q_x}{\partial x} + \frac{\partial Q_y}{\partial y} + q + N_x\frac{\partial^2 w}{\partial x^2} + \\ &\qquad N_y\frac{\partial^2 w}{\partial y^2} + 2N_{xy}\frac{\partial^2 w}{\partial x \partial y} = 0 \\ &\frac{\partial M_x}{\partial x} - \frac{\partial M_{xy}}{\partial y} - Q_x = 0 \\ &\frac{\partial M_y}{\partial y} - \frac{\partial M_{xy}}{\partial x} - Q_y = 0 \end{aligned}\right\} \quad (1)$$

The five foregoing equations contain eight unknowns, N_x, N_y, N_{xy}, M_x, M_y, M_{xy}, Q_x, and Q_y. More equations will be obtained through the use of the variational theorem of complementary energy in conjunction with Lagrangian multipliers.

The strain energy of the two face layers is given by the following expression:

$$V_f = \frac{1}{2}\iint \frac{1}{2Et}\left[N_x^2 + N_y^2 - 2\nu N_x N_y + 2(1+\nu)N_{xy}^2\right] + \frac{2}{Et(h+t)^2}\left[M_x^2 + M_y^2 - 2\nu M_x M_y + 2(1+\nu)M_{xy}^2\right] + \left[N_x\left(\frac{\partial w}{\partial x}\right)^2 + N_y\left(\frac{\partial w}{\partial y}\right)^2 + 2N_{xy}\frac{\partial w}{\partial x}\frac{\partial w}{\partial y}\right]\Bigg\} dx\,dy$$

The strain energy stored in the core is given by

$$V_c = \frac{1}{2h}\iint\left[\frac{Qx^2}{G_{xz}} + \frac{Qy^2}{G_{yz}}\right] dx\,dy$$

The work done by the surface forces over that portion of the surface where the displacements are prescribed is given by

$$W = \int_{-b/2}^{b/2}\left[N_x u + N_{xy}v + \left(N_x\frac{\partial w}{\partial x} + N_{xy}\frac{\partial w}{\partial y} + Q_x\right)\times w + M_x\beta + M_{xy}\gamma'\right]_{x=a/2,\ x=-a/2} dy + \int_{-a/2}^{a/2}\left[N_y v + N_{xy}u + \left(N_y\frac{\partial w}{\partial y} + N_{xy}\frac{\partial w}{\partial x} + Q_y\right)w + M_y\gamma + M_{xy}\beta'\right]_{y=b/2,\ y=-b/2} dx$$

In order to render the complementary energy $(V_f + Vc - W)$ a minimum subject to the equations of equilibrium (1), these equations are multiplied by Lagrangian multipliers λ_1, λ_2, λ_3, λ_4, and λ_5, respectively, and then integrated over the area of the plate. This result is added to the complementary energy, the first variation of the resulting expression is carried out with respect to the unknown functions N_x, N_y, N_{xy}, M_x, M_y, M_{xy}, Q_x, and Q_y, and the result is set equal to zero:

$$\delta V_f + \delta V_c - \delta W + \delta\iint\Bigg[\lambda_1\left(\frac{\partial N_x}{\partial x} + \frac{\partial N_{xy}}{\partial y}\right) + \lambda_2\left(\frac{\partial N_y}{\partial y} + \frac{\partial N_{xy}}{\partial x}\right) + \lambda_3\left(\frac{\partial Q_x}{\partial x} + \frac{\partial Q_y}{\partial y} + q + N_x\frac{\partial^2 w}{\partial x^2} + N_y\frac{\partial^2 w}{\partial y^2} + 2N_{xy}\frac{\partial^2 w}{\partial x \partial y}\right) + \lambda_4\left(\frac{\partial M_x}{\partial x} - \frac{\partial M_{xy}}{\partial y} - Q_x\right) + \lambda_5\left(\frac{\partial M_y}{\partial y} - \frac{\partial M_{xy}}{\partial x} - Q_y\right)\Bigg] dx\,dy = 0$$

Received February 3, 1964; revision received July 8, 1964.
* Associate Professor of Engineering.